The electrode-electrolyte interface in CO2 reduction and H2 evolution: a multiscale approach

Cecilio de Oliveira Monteiro, M

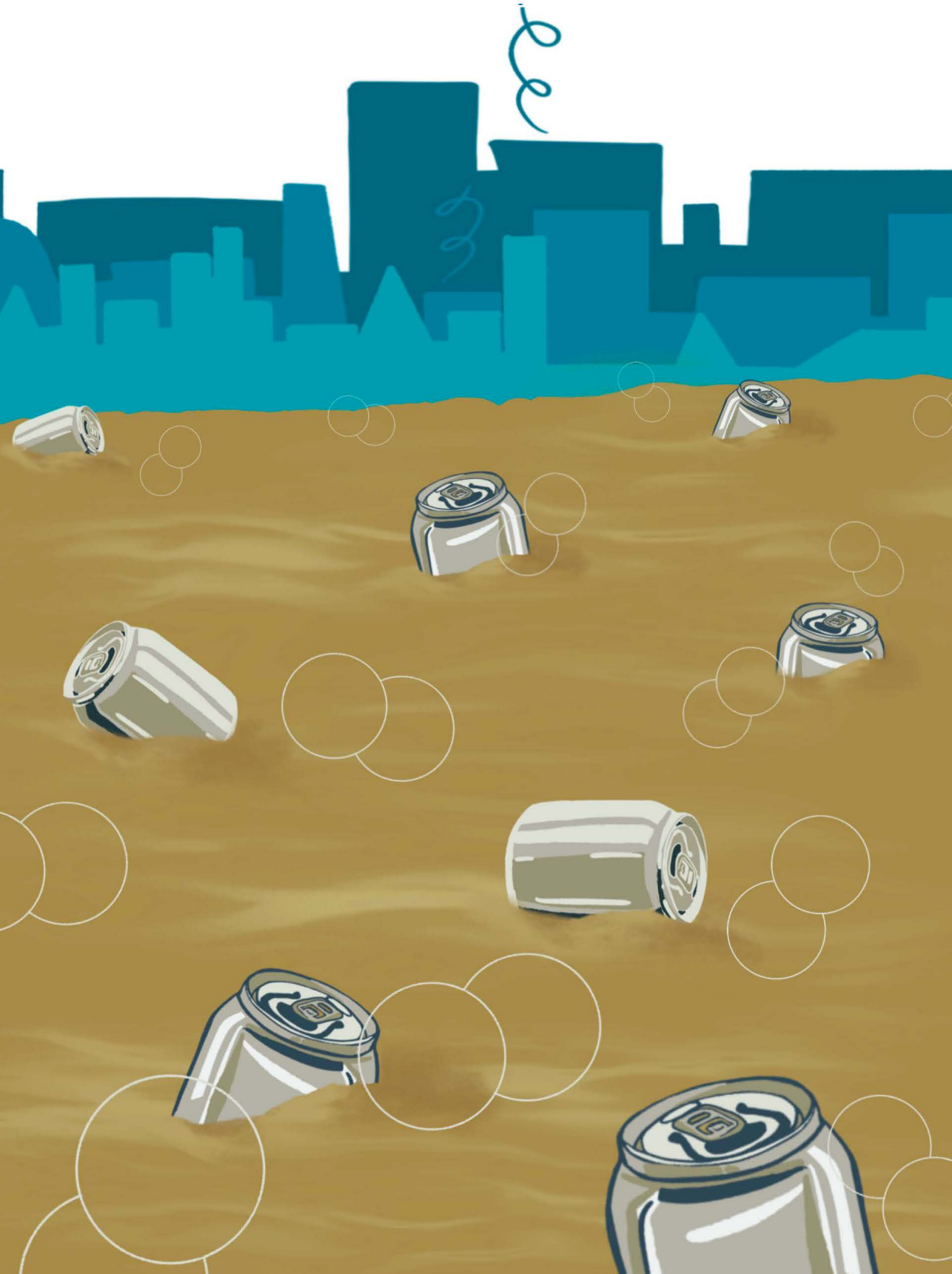

7

Alumina contamination through polishing and its effects on hydrogen evolution on gold electrodes

This chapter is based on Monteiro, M. C. O., Koper, M. T. M. *Electrochimica Acta, 325*, 134915 (2019)

Abstract

In this Chapter we show how the contamination of gold electrodes with alumina particles by electrode polishing leads to an enhancement in activity for hydrogen evolution (HER) in neutral media. Polishing is one of the most used electrode treatments, however, we show that particles from the polishing media cannot be easily removed from the electrode surface by standard cleaning procedures. Comparing the HER activity of gold disc electrodes polished with either diamond suspension or alumina paste, we show that the latter leads to higher current densities, specifically for the water reduction to hydrogen. A similar enhancement in HER activity was observed by the addition of Al^{3+} cations to the electrolyte, demonstrating that the particles are not catalytically active, but that the Al^{3+} species released in solution due to corrosion promote the water reduction reaction. Due to an increase in the local OH^- concentration during HER, the contaminating Al^{3+} cations precipitate and may deposit at the electrode surface as $Al(OH)_3$. In the presence of a high enough Al^{3+} concentration, layered $Al(OH)_3$ plates cover the whole electrode surface. The plates are composed of $Al(OH)_3$ sheets intercalated by sulphate anions. Surprisingly, the $Al(OH)_3$ sheets do not affect the gold blank voltammetry, and therefore remain undetected by simple electrochemical characterization methods.

7.1 Introduction

Gold electrocatalysts are widely studied for several oxidation[1] and reduction reactions[2–9], among which CO_2 reduction and the competing hydrogen evolution have gained a lot of attention recently.[10–12] Understanding these reactions at the atomistic level is key to the design and optimization of larger-scale processes. In fundamental electrocatalysis studies, electrodes are usually pre-treated, in order to obtain a clean, homogeneous and reproducible surface. The most common pre-treatments used for gold electrodes are: mechanical polishing, chemical etching, electropolishing, annealing, or a combination thereof.[13–15] However, the influence of different pre-treatments on the stability, structure, composition, and catalytic activity of gold electrodes is not well documented. Actually, most studies overlook the possibility of such an influence and do not report a detailed characterization of the pre-treated electrodes.

Flame annealing is the most reliable method to prepare electrodes and leads to a clean and (re)ordered surface. It allows, for example, the preparation of single crystals without the need of UHV techniques.[16] Polycrystalline electrodes, on the other hand, are usually cut from metal foils and require mechanical polishing to prepare a smooth, clean and reproducible surface.[17] The quality of the polishing procedure also directly influences the quality of the surface after subsequent flame annealing. In addition, not all kind of electrodes can be flame annealed, such as rotating disc electrodes (when embedded in Teflon holders) or microelectrodes. Metals such as copper cannot be flame annealed in air without avoiding surface oxidation.[18]

Even though electrode polishing is a well-known procedure, it has been reported that even when following standard polishing/cleaning procedures, particle residues from the polishing media can remain on the electrode surface even after rinsing extensively with water or after subjecting to ultra-sonication.[19–22] Polishing pastes and suspensions contain alumina, diamond, silicon carbide or boron carbide powders, depending on the application. The extent of the contamination and how it affects electrochemical and especially electrocatalytic processes is expected to vary depending on the polishing media used.

There are only a few indications in the literature that polishing with alumina influences electrocatalysis, although the effect of trace metal contaminants on hydrogen evolution on gold have been previously reported.[23,24] Jacobse et al. demonstrated that platinum ultra-micro electrodes (UME) polished with alumina have lower catalytic activity than flame annealed UMEs.[25] The effect is attributed to

contamination of the UMEs either due to the preparation method or impurities in the chemicals used. On the other hand, Volpe et al. showed that the mechanical polishing of PtBi catalysts with alumina, instead of diamond, leads to larger activity towards formic acid oxidation.[26] Clark et al. also pointed out that alumina residues could be problematic when studying CO_2 reduction on copper, as metallic aluminium is an active catalyst for the competing hydrogen evolution reaction (HER).[27] However, no further investigations were carried out in this regard. Studies regarding the effect of gold surface pre-treatments have mainly been carried out in the field of biomaterials. It has been demonstrated that the surface preparation method strongly influences the self-assembly of organic molecules due to changes in the surface roughness and cleanliness.[28–31] However, the implications of these treatments on the gold catalytic activity has not been thoroughly investigated.

In this Chapter, we study the effect of the polishing media on the electrocatalytic activity of gold electrodes towards HER. We have chosen this model system, due to its relevance as a competing reaction in different electrocatalytic processes that take place (in aqueous media) at potentials below 0 V vs. RHE. Surprisingly, the presence of alumina particles leads to a significant increase in the gold catalytic activity for HER, even though the presence of alumina remains undetected by standard blank cyclic voltammetry. To investigate this enhancement in reactivity, the electrode structure and composition is studied by using a combination of blank voltammetry, Scanning Electron Microscopy (SEM), and Energy Dispersive X-Ray Spectrometry (EDX) both before and after the electrocatalytic experiments. The results demonstrate that the enhancement is due to the corrosion products from the alumina polishing particles that are released into the electrolyte.

7.2 The effect of the polishing media on HER

Polycrystalline gold electrodes polished with either alumina or diamond paste were subsequently cleaned by ultra-sonication and flame annealing before being characterized by cyclic voltammetry (CV). Recording CVs from 0 to 1.75 V vs. RHE is a standard way to characterize polycrystalline gold electrodes.[32] It provides information about the electrochemical active surface area (ECSA) through the charge associated with the gold reduction peak. Gold is considered an ideal electrode for fundamental studies, due to its extensive double layer region (from 0 to 1.3 vs. V vs. RHE in acid) and weak chemisorption of species in comparison to Pt, for example.[33] As depicted in Fig. 7.1 independent of the polishing media used

(alumina or diamond), the gold displays a similar broad oxidation peak, starting at 1.35 V vs. RHE. During the backward scan, one sharp reduction peak is observed at 1.18 V vs. RHE, related to the reduction of the formed gold oxide layer. The double layer region, between 0.1 and 1.3 V vs. RHE, does not change significantly with the polishing media. Minor differences in ECSA can be observed, although repeated experiments show that these are not related to the polishing media, but to using different electrodes.

Even though the CVs of the gold electrodes polished with diamond or alumina look similar, observation of the electrodes under a Scanning Electron Microscope (SEM) shows that a considerable number of particles remains at the surface even after carrying out the standard cleaning procedures described in the Methods section (Appendix D). As can be seen in the SEM images from Fig. 7.2b, samples polished with alumina get contaminated with particles of various sizes (from 100 nm to 3 μm). Additional SEM images at different magnifications can be found in Fig. D.1a and Fig. D.1b in Appendix D and show that the alumina particles are evenly distributed over the whole surface. In the case of diamond (Fig. 7.2a), mainly large and randomly spaced particles can be found, in much smaller amounts compared to alumina. The line structure observed in Fig. 7.2a on the flat region is believed to be soot, formed during flame annealing. The elemental composition of the particles was investigated by EDX. Line scans through the particles found in the alumina polished sample show that the gold signal intensity decreases when the beam approaches the particles while the aluminium and oxygen signals increase (Fig. 7.2b). This shows that the particles come from the polishing media and are ascribed to Al_2O_3. The Al/O ratio does not agree with the stoichiometry, because of the different interaction depths for different elements (resolution of the technique) and the standardless quantification method used.[34] For a given beam energy, the interaction volume will decrease with increasing atomic number. EDX line scans performed on the diamond polished electrode show that through the particles, the carbon signal increases as the gold signal decreases, whereas no signal for oxygen is observed (Fig. 7.2a). Again, it is confirmed that the particles come from the diamond suspension. It is important to point out that trace amounts of carbon are found in all the samples, due to beam-induced hydrocarbon contamination (both from the instrument and from the sample).[35] The amount of carbon found will depend, for example, on the period of time the beam interacts with the surface and

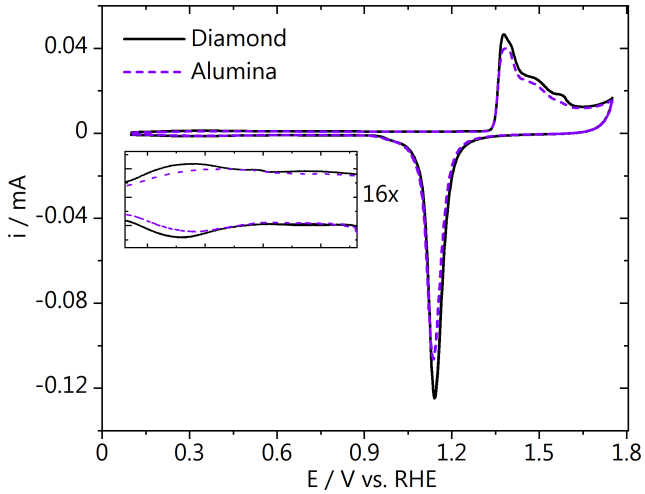

Fig. 7.1. Cyclic voltammetry of polycrystalline gold electrodes polished with either alumina or diamond suspension in 0.1 M H_2SO_4 taken at a scan rate of 50 mV s^{-1}. The inset shows part of the gold double layer region.

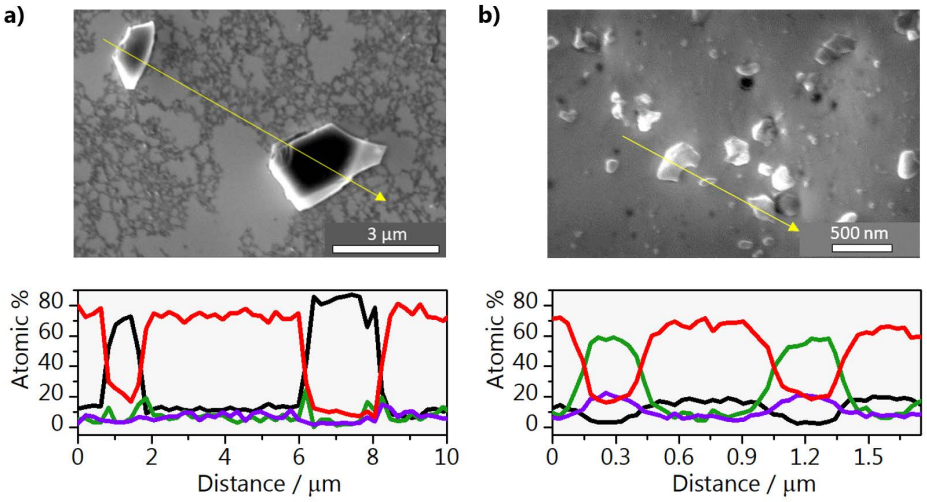

Fig. 7.2. SEM micrographs and EDX line spectra of gold electrodes after polishing with **a)** diamond and **b)** alumina. The lines refer to the following signals: (—) C K, (—) O K, (—) Al K and (—) Au M.

the acceleration voltage. The carbon contamination cannot be detected by cyclic voltammetry characterization.

According to suppliers of polishing media, gold should be polished with diamond suspensions down to 1 µm and the last polishing step should be carried out with alumina paste (0.05 µm).[36] However, they also mention that soft metals like gold are highly prone to diamond embedding. In most work found in literature (including the ones cited in this paper), alumina is the polishing medium of choice for gold electrodes. This is because it is easier to obtain a scratch free, mirror-like finish polishing with alumina than with diamond. It is also important to point out that the surface preparation not only influences the surface morphology but also the reproducibility of electrochemical experiments and the surface cleanliness. In the present work we have only polished and flame annealed the gold electrode, in order to avoid contamination and to have the best reproducibility. A brief explanation on how other treatments, such as chemical etching and electropolishing, affect the surface as well as SEM micrographs can be found in Fig. D.2 in Appendix D, along with a more detailed reasoning of the electrode preparation method chosen for this work.

Considering the large number of polishing particles that remain on the electrode surface even after the standard cleaning procedures, it is surprising that their blank voltammetry is practically identical (see Fig. 7.1). To probe if the particles can influence electrochemical reactions, we have performed HER experiments. Fig. 7.3 shows the curves obtained for HER on gold electrodes polished with either diamond or alumina in the pH = 3 Li_2SO_4 electrolyte. Surprisingly, a significant increase in current density is observed for the alumina polished sample, especially at potentials below –0.8 V vs. RHE. The voltammogram clearly has two different regions. The first cathodic peak observed between 0 and –0.7 V vs. RHE, is attributed to the reduction of protons ($2H^+ + 2e^- \rightarrow H_2$).[37] A peak in the current is observed because the reaction rate is limited by diffusion of protons towards the surface. As the diffusion layer thickness increases and the local pH becomes more alkaline, a proton concentration gradient is built up. The peak current depends on the proton concentration in the electrolyte. In the second region, between –0.8 and –1 V vs. RHE, the reduction of water takes place ($2H_2O + 2e^- \rightarrow H_2 + 2OH^-$).

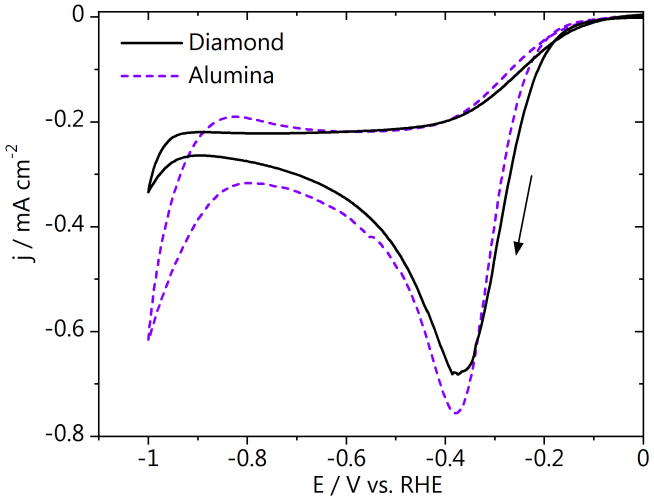

Fig. 7.3. Cyclic voltammogram of hydrogen evolution on gold electrodes polished with alumina or diamond. CVs were recorded in 0.1 M Li_2SO_4 (argon saturated, pH = 3) and taken at a scan rate of 50 mV s^{-1}.

Based on the curves shown in Fig. 7.3, the reduction of H_2O is more affected by the alumina contamination than the reduction of protons. The latter is also confirmed by calculating the Tafel slopes. For proton reduction 101 and 100 mV dec^{-1} were found for the alumina and diamond polished samples, respectively. For water reduction, a lower Tafel slope was found for the alumina polished sample in comparison to the diamond polished sample. The topography and composition of the electrodes was also observed in the SEM directly after the HER experiments. SEM micrographs and EDX spectra can be found in Fig. D.3 in Appendix D. These data show the same situation as shown in Fig. 7.2, i.e. the electrocatalytic experiments have no significant influence on the density, size, and composition of the contaminating polishing particles. In addition, the sulphur signal was also monitored in the EDX line scans after HER, as the reaction was carried out in a sulphate containing electrolyte. However, no significant S signal could be determined.

7.3 Addition of Al^{3+} to the electrolyte

To elucidate why the HER activity increases in the presence of alumina particles, it is necessary to understand how stable these particles are in solution at different pH. According to the Pourbaix diagram of aluminium[38], at pH values below 4 and potentials between –1.69 and 1.9 V vs. RHE, alumina (Al_2O_3) undergoes

corrosion leading to the release of Al^{3+} ions in solution through the following reaction: $Al_2O_3{\cdot}H_2O + 6H^+ \rightarrow 2Al^{3+} + 4H_2O$. It has been shown that alkaline earth cations can strongly influence hydrogen evolution, although the exact mechanism behind it is not yet fully understood.[39] To observe if Al^{3+} has an effect on HER, different amounts of $Al_2(SO_4)_3$ were added to the background electrolyte (0.1 M Li_2SO_4). The gold electrode was polished with diamond, flame annealed and characterized before each addition experiment. The characterization CVs before HER can be found in Fig. D.4 in Appendix D, where a very reproducible surface was obtained by flame annealing prior to each run. Fig. 7.4a shows the HER current densities obtained in the presence of different concentrations of $Al_2(SO_4)_3$ in the electrolyte. An increase in the water reduction current is observed, which strongly indicates that the aluminium ions released in solution (due to corrosion of the alumina particles) are responsible for the enhancement in the HER activity on gold. In addition, it can also be seen in Fig. 7.4a that high concentrations of aluminium cations (above 250 μM Al^{3+}) lead to a second reduction peak at –0.6 V vs. RHE. It is important to point out that the observed current cannot be due to aluminium plating on the gold electrode. The charge associated with the deposition of a full monolayer of aluminium on the electrode would be much lower than obtained, in the order of 600 μC cm^{-2}. In addition, the potential window used is above the equilibrium reduction potential of Al^{3+} at pH = 3 (–1.6934 V). Based on the CVs displayed in Fig. 7.4a, we estimate that the corrosion of the alumina particles during the experiment from Fig. 7.3 leads to an Al^{3+} concentration of less than 50 μM (near the electrode surface). The Tafel slopes were calculated and at high overpotentials, where the activity for water reduction is higher, the Tafel slope decreases 30 mV dec^{-1} in the presence of micro molar concentrations of Al^{3+}. This difference underpins how strongly the Al^{3+} cations affect HER. The gold sample was also characterized after the last HER experiment was performed (with the addition of 500 μM $Al_2(SO_4)_3$). The cyclic voltammograms can be found in Fig. D.5a in Appendix D, showing no apparent changes in the gold blank voltammetry. However, by subsequently analysing the electrode with SEM and EDX (Fig. 7.4b), flakes were found on the surface. Through EDX, it can be seen that these flakes are composed of aluminium and oxygen. A SEM micrograph taken at lower magnification can be found in Appendix D (Fig. D.5b) and shows how homogeneously distributed the deposits are.

Considering the speciation diagram of aluminium (see Fig. D.6a) in Appendix D), at pH above 5 and at high enough Al^{3+} concentration, Al^{3+} precipitates as

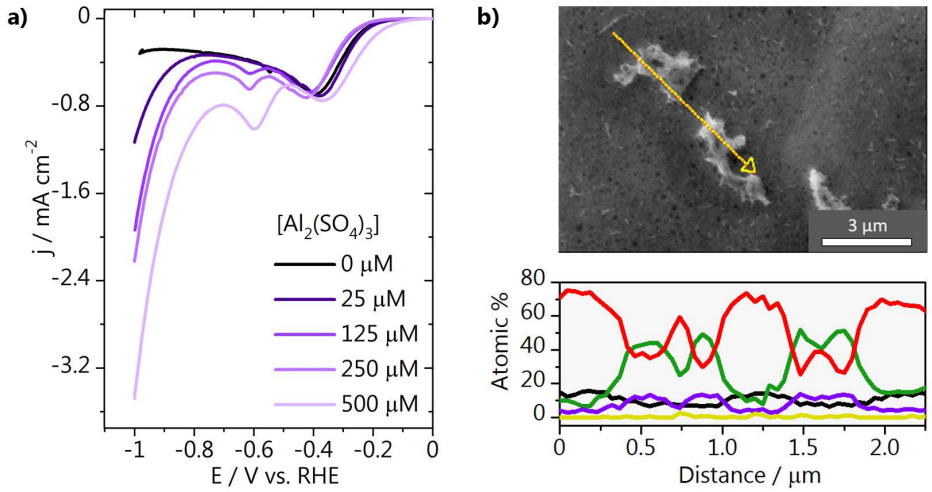

Fig. 7.4. a) Cyclic voltammogram of hydrogen evolution on gold electrodes polished with diamond. CVs were recorded in 0.1 M Li_2SO_4 (argon saturated) at a scan rate of 50 mV s^{-1}. For each curve, different amounts of 0.01 M $Al_2(SO_4)_3$ were added to the electrolyte. Each experiment was done with a fresh electrolyte mixture with a freshly prepared electrode. **b)** SEM micrographs and EDX line spectra of gold electrodes after hydrogen evolution in 0.1 M Li_2SO_4 (argon saturated) with the addition of 500 µM $Al_2(SO_4)_3$. The lines refer to the following signals: (—) C K, (—) O K, (—) Al K, (—) Au M and (—) S K.

$Al(OH)_3$. Even though the bulk pH of our experiments is acidic (pH = 3), during HER, the pH at the electrode surface will be more alkaline. This creates the required environment for $Al(OH)_3$ precipitation. The fact that Al^{3+} can deposit on the surface as hydroxide at increased local pH also means that if an electrode is contaminated with alumina particles and used for experiments during a whole day, the surface composition will not be reproducible throughout all the measurements. As previously shown, these differences will not be apparent in the blank cyclic voltammetry.

To further confirm that Al^{3+} deposits at the electrode surface as aluminium hydroxide during HER, the reaction was also performed on a gold electrode polished with diamond in 0.01 M pure $Al_2(SO_4)_3$. The electrolyte concentration here is lower than in the previous experiments, due to the slow dissolution kinetics of the aluminium salt. Fig. 7.5 shows the CVs for HER in pure $Al_2(SO_4)_3$, together with the curves from Fig. 7.3 for comparison. Larger current densities are obtained in the pure Al^{3+} containing electrolyte, in comparison with HER performed in pure Li_2SO_4. These results are in agreement with Fig. 7.4a, where the addition of small amounts of Al^{3+} to the background electrolyte lead to a 3-fold increase in the HER current

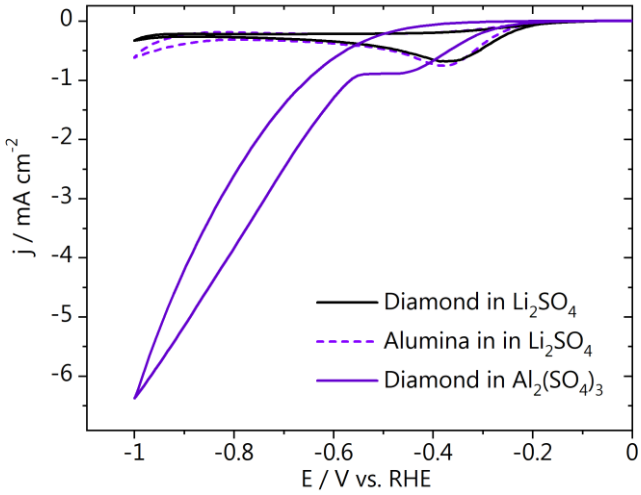

Fig. 7.5. Cyclic voltammogram of hydrogen evolution on gold polished with diamond paste taken at a scan rate of 50 mV s^{-1} in 0.01 M $Al_2(SO_4)_3$ (argon saturated, pH = 2.7). The CVs from Fig. 7.3 are added for comparison.

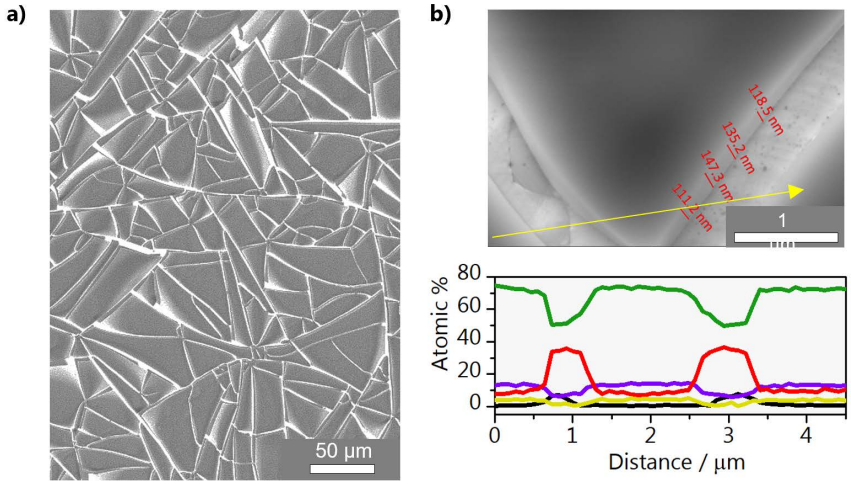

Fig. 7.6. a) SEM micrographs and **b)** EDX line spectra of the gold electrode after hydrogen evolution in 0.01 M $Al_2(SO_4)_3$. The lines refer to the following signals: (—) C K, (—) O K, (—) Al K, (—) Au M and (—) S K.

density. After the HER experiment, SEM and EDX were performed in order to characterize the electrode topography and composition. As shown in Fig. 7.6a, after HER in pure $Al_2(SO_4)_3$, the electrode was fully covered with an aluminium hydroxide layer. Plates, in average 128 ±14 nm thick, are present on the surface with the spacing in between them ranging from 1 to 3 μm. According to EDX (Fig. 7.6b) they are composed of Al, O, and S, but a low signal for gold is still obtained. As previously mentioned, the latter is due to the depth resolution of the technique compared to the hydroxide layer thickness. The region in between the plates is composed of Al, O and again Au, however no sulphur was detected (see Fig. D.7 in Appendix D). The presence of sulphur in the plates as well as their morphology leads to the conclusion that they are layered aluminium hydroxide sheets. The planar sheets are composed by alumina octahedrons, where each aluminium ion shares 3 pairs of OH^- with 3 other Al^{3+}. They are intercalated, in this case, with sulphate ions. See the top and side view of the $Al(OH)_3$ sheets molecular structure in Appendix D (Fig. D.6). Our findings are also supported by comparison with the work of Guo et al.[40] where zinc and aluminium double layered hydroxides were synthesized and the aluminium layer has similar morphology as we obtained (Fig. 7.6a). The gold electrode was also characterized by cyclic voltammetry before and after the hydroxide layer was present on the surface. Surprisingly, the gold CVs nearly overlap (see Fig. D.8 in Appendix D), which not only indicates that the hydroxide plates do not affect the apparent electrochemically active surface area, but are highly porous, so that species in the electrolyte can easily reach the gold surface.

Considering that the voltammetry of the gold was unaltered in the presence of the aluminium hydroxide layer, the activity of this Au-$Al(OH)_3$ modified electrode was also tested for HER. Results can be seen in Fig. 7.7 and show that the HER current for both proton and water reduction obtained during the first cycle is equivalent to that obtained when the electrode is contaminated with alumina particles. During subsequent cycles, two proton reduction peaks are observed and the current due to water reduction increases, indicating that the concentration of Al^{3+} in the vicinity of the electrode surface is also increasing. It is important to notice that during cycles 2 to 5 the proton reduction peak keeps decreasing, likely because of a gradual increase in the local pH. This is expected, as in the presence of the layered hydroxide on the surface, compared to the bare gold, species will take longer to diffuse in and out of the pores. Again, after these HER experiments, the CV of the gold electrode remains unaltered (see Fig. D.8 in Appendix D).

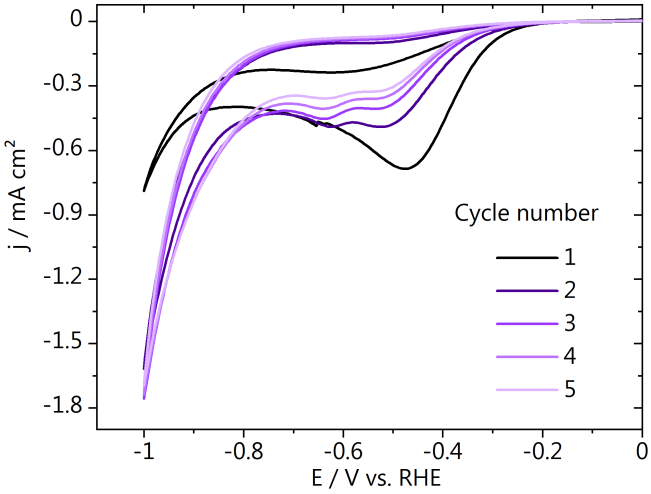

Fig. 7.7. Cyclic voltammogram of hydrogen evolution on gold-$Al(OH)_3$ modified electrode taken at a scan rate of 50 mV s^{-1} in 0.1 M Li_2SO_4 (Argon saturated, pH = 3).

7.4 Alumina removal from the surface

Contaminating alumina particles can of course be removed, by also removing layers of gold. However, for full removal, many electrochemical etching cycles are required. In Fig. D.9 in Appendix D we show that after 2 etching cycles of 1 min in 0.1 M H_2SO_4 (normally 1 etching cycle is performed, for 20 seconds), increased activity for HER is still found. A more detailed discussion on the advantages and disadvantages of prolonged etching is available in Appendix D. Other surface cleaning methods can also be effective for the removal of the polishing contaminants as, for example, sputtering. However, this technique requires ultra-high vacuum (UHV) experiments, which significantly complicates the experimental setup. Thus, mechanical polishing is still the most common surface preparation method in electrochemical studies. Based on the data shown in this work, we believe that a diamond suspension is a safer polishing medium (even though it might lead to a worse surface finish) than alumina, to completely avoid affecting the catalytic activity of electrodes. However, if alumina is employed and only the standard cleaning procedures are performed (mild etching and flame annealing), it is important to be aware that alumina particles on electrode surface corrode in acidic media and release Al^{3+} in the electrolyte. The latter is of extreme importance as cations have shown to influence not only hydrogen evolution but also reactions like CO_2[41] and CO reduction[42], oxygen evolution[43], oxygen reduction, methanol oxidation, among others.[44,45,46] It is also important to highlight that the presence of

surface contaminants cannot be clearly seen by electrochemical characterization of the electrode. Therefore, it is advisable to always use complementary techniques like SEM and EDX to evaluate the surface morphology and composition, no matter which surface pre-treatment was employed.

7.5 Conclusions

Even though polishing is a common electrode preparation method, it may have profound effects on the electrochemical and electrocatalytic reactivity of the electrode. In the present work, we have polished gold samples with either diamond or alumina and evaluated how the polishing medium influences the catalytic activity for hydrogen evolution in mildly acidic electrolyte solutions. Results show that polishing with alumina, despite subsequent electrode cleaning, leads to contamination of the surface with Al_2O_3 particles. Polishing with diamond also leads to contamination, but with significantly fewer particles remaining on the surface. The gold electrodes polished with alumina show higher activity for the water reduction reaction than the ones polished with diamond, due to corrosion of the alumina particles and release of Al^{3+} cations in the electrolyte. The former was confirmed by an increase in HER currents for an electrode polished with diamond, when adding micro molars of Al^{3+} to the background electrolyte. The cations influence water reduction much stronger than proton reduction. Furthermore, we show that by observing the aluminium speciation diagram, it is possible to predict at which pH and applied potentials alumina particles will undergo corrosion or not. We also found that due to an increase in the local pH during HER, even small amounts of Al^{3+} cations deposit on the gold surface as $Al(OH)_3$. At high concentrations (pure Al^{3+} containing electrolyte) layered hydroxides are formed, intercalated with sulphate anions. The alumina contamination can be remediated by the removal of gold layers, which can be achieved by chemical etching, for example. However, several etching cycles are necessary for complete removal and can significantly increase the surface roughness. We hope that our work raises awareness of the potential effects of surface preparation and contamination. This becomes crucial, for example, when studying electrolyte effects on electrochemical reactions. Cations do not only have an effect on hydrogen evolution, but also on many other electrochemical reactions. Therefore, when working in acidic and neutral media, we recommend to polish electrodes with diamond suspensions or other stable polishing media.

References

(1) Burke, L. D.; Nugent, P. F. *Gold Bull.* 1998, *31* (2), 39–50.
(2) Nazemi, M.; Panikkanvalappil, S. R.; El-Sayed, M. A. *Nano Energy* 2018, *49*, 316–323.
(3) Qin, Q.; Heil, T.; Antonietti, M.; Oschatz, M. *Small Methods* 2018, *2* (12), 1800202.
(4) Yao, Y.; Zhu, S.; Wang, H.; Li, H.; Shao, M. *J. Am. Chem. Soc.* 2018, *140* (4), 1496–1501.
(5) El-Deab, M. S.; Okajima, T.; Ohsaka, T. *J. Electrochem. Soc.* 2003, *150* (7), A851.
(6) Sarapuu, A.; Nurmik, M.; Mändar, H.; Rosental, A.; Laaksonen, T.; Kontturi, K.; Schiffrin, D. J.; Tammeveski, K. *J. Electroanal. Chem.* 2008, *612* (1), 78–86.
(7) Laforgue, A.; Addou, T.; Bélanger, D. *Langmuir* 2005, *21* (15), 6855–6865.
(8) Das, J.; Aziz, M. A.; Yang, H. *J. Am. Chem. Soc.* 2006, *128* (50), 16022–16023.
(9) Damian, A.; Omanovic, S. *J. Mol. Catal. A Chem.* 2006, *253* (1–2), 222–233.
(10) Zhao, S.; Jin, R.; Jin, R. *ACS Energy Lett.* 2018, *3* (2), 452–462.
(11) Zhang, B. A.; Ozel, T.; Elias, J. S.; Costentin, C.; Nocera, D. G. *ACS Cent. Sci.* 2019, *5*, acscentsci.9b00302.
(12) Rodriguez, P.; Koper, M. T. M. *Phys. Chem. Chem. Phys.* 2014, *16* (27), 13583–13594.
(13) Ahrens, P.; Zander, M.; Hasse, U.; Wulff, H.; Jeyabharathi, C.; Kruth, A.; Scholz, F. *ChemElectroChem* 2018, *5* (6), 943–957.
(14) Jarosz, M.; Kapusta-Kołodziej, J.; Jaskuła, M.; Sulka, G. D. *J. Nanomater.* 2015, *2015*.
(15) Hamelin, A. *J. Electroanal. Chem.* 1996, *407* (1), 1–11.
(16) Clavilier, J. In *Journal of the American Chemical Society*; Wieckowski, A., Ed.; CRC Press, 2000; Vol. 122, pp 6139–6139.
(17) Samuels, L. E. 4th ed.; ASM International: Ohio, 2003.
(18) Tahir, D.; Tougaard, S. *J. Phys. Condens. Matter* 2012, *24* (17), 175002.
(19) Zhang, L. *J. Electrochem. Soc.* 1999, *146* (4), 1442.
(20) Kiema, G. K.; Aktay, M.; McDermott, M. T. *J. Electroanal. Chem.* 2003, *540*, 7–15.
(21) Kamau, G. N.; Willis, W. S.; Rusling, J. F. *Anal. Chem.* 1985, *57* (2), 545–551.
(22) Kazee, B.; Weisshaar, D. E.; Kuwana, T. *Anal. Chem.* 1985, *53* (13), 2736–2739.
(23) Solla-gullón, J.; Aldaz, A.; Clavilier, J. *J. Electroanal. Chem.* 2017, *793*, 41–47.
(24) Solla-gullón, J.; Aldaz, A.; Clavilier, J. *Electrochim. Acta* 2013, *87*, 669–675.
(25) Jacobse, L.; Raaijman, S. J.; Koper, M. T. M. *Phys. Chem. Chem. Phys.* 2016, *18* (41), 28451–28457.
(26) Volpe, D.; Casado-Rivera, E.; Alden, L.; Lind, C.; Hagerdon, K.; Downie, C.; Korzeniewski, C.; DiSalvo, F. J.; Abruña, H. D. *J. Electrochem. Soc.* 2004, *151* (7), A971.
(27) Clark, E. L.; Resasco, J.; Landers, A.; Lin, J.; Chung, L. T.; Walton, A.; Hahn, C.; Jaramillo, T. F.; Bell, A. T. *ACS Catal.* 2018, *8* (7), 6560–6570.
(28) Ho, L. S. J.; Limson, J. L.; Fogel, R. *ACS Omega* 2019, *4* (3), 5839–5847.
(29) Carvalhal, R. F.; Freire, R. S.; Kubota, L. T. *Electroanalysis* 2005, *17* (14), 1251–1259.
(30) Tkac, J.; Davis, J. J. *J. Electroanal. Chem.* 2008, *621* (1), 117–120.
(31) Hoogvliet, J. C.; Dijksma, M.; Kamp, B.; Van Bennekom, W. P. *Anal. Chem.* 2000, *72* (9), 2016–2021.
(32) Do, U. P.; Seland, F.; Johannessen, E. A. *J. Electrochem. Soc.* 2018, *165* (5), H219–H228.
(33) Xue, S.; Garlyyev, B.; Watzele, S.; Liang, Y.; Fichtner, J.; Pohl, M. D.; Bandarenka, A. S. *ChemElectroChem* 2018, *5* (17), 2326–2329.
(34) Burke, L. D.; Nugent, P. F. *Gold Bull.* 1997, *30* (i), 43–53.
(35) Feliu, J. M.; Herrero, E. *Contrib. Sci.* 2010, *6* (2), 161–172.
(36) Lowe, B. G. In *Introduction to Energy Dispersive X-ray Spectrometry (EDS)*; Goldstein, J., Ed.; Springer Science & Business Media, 2012; p 372.

(37) Vladar, A.; Postek, M. *Microsc. Microanal.* 2005, *11* (S02), 764–765.
(38) Buehler, SUMMET method for gold https://www.buehler.com/sumMet.php?material=Gold (accessed Jul 16, 2019).
(39) Kahyarian, A.; Brown, B.; Nesic, S. *J. Electrochem. Soc.* 2017, *164* (6), H365–H374.
(40) Ashby, M. F.; Jones, D. R. H. 4th ed.; Elsevier Ltd., 2012.
(41) Guo, X.; Xu, S.; Zhao, L.; Lu, W.; Zhang, F.; Evans, D. G.; Duan, X. *Langmuir* 2009, *25* (17), 9894–9897.
(42) Resasco, J.; Chen, L. D.; Clark, E.; Tsai, C.; Hahn, C.; Jaramillo, T. F.; Chan, K.; Bell, A. T. *J. Am. Chem. Soc.* 2017, *139* (32), 11277–11287.
(43) Pérez-Gallent, E.; Marcandalli, G.; Figueiredo, M. C.; Calle-Vallejo, F.; Koper, M. T. M. *J. Am. Chem. Soc.* 2017, *139* (45), 16412–16419.
(44) Zaffran, J.; Stevens, M. B.; Trang, C. D. M.; Nagli, M.; Shehadeh, M.; Boettcher, S. W.; Caspary Toroker, M. *Chem. Mater.* 2017, *29* (11), 4761–4767.
(45) Herranz, J.; Durst, J.; Fabbri, E.; Patru, A.; Cheng, X.; Permyakova, A. A.; Schmidt, T. J. *Nano Energy* 2016, *29*, 4–28.
(46) Strmcnik, D.; Kodama, K.; Van Der Vliet, D.; Greeley, J.; Stamenkovic, V. R.; Marković, N. M. *Nat. Chem.* 2009, *1* (6), 466–472.